Modeling Drop Generation at the Microscale

M. S. Hanchak[1] and E. P. Furlani[2]

[1]Graphic Communications Group, Eastman Kodak Company
3000 Research Blvd, Dayton, OH 45420

[2]Eastman Kodak Research Laboratories
1999 Lake Avenue, Rochester, New York 14650-2216
Office: (585) 588-0344 Fax: (585) 588-5987
edward.furlani@kodak.com

ABSTRACT

We present a numerical model for predicting drop generation for microfluidic printing applications. The model is based on a slender-jet approximation and involves the solution of coupled nonlinear partial differential equations for predicting jet instability and drop formation. The novelty of the model is that it predicts jet instability to breakup and beyond thereby enabling an analysis of the generation of multiple sequential drops including the details of satellite formation. The key advantages of the model are its ease of implementation and speed of computation, which is several orders of magnitude faster than CFD analysis. The model is demonstrated via application to high-speed continuous inkjet printing.

Keywords: slender jet analysis, microdrop generation, continuous inkjet printing, microfluidic printing, microjet instability, Marangoni instability

1 INTRODUCTION

Research into the phenomenon of jet breakup and drop formation has increased dramatically over the last several years, due in part to rapid advances in microfluidic, biomedical, and nanoscale technologies [1,2]. Novel applications are proliferating, especially in fields that benefit from high-speed and low-cost patterned deposition of discrete droplets of micro- or nanoscale materials. Emerging applications in this field include printing functional materials for flexible electronics, microdispensing of biochemicals, printing biomaterials (e.g. cells, genetic material), and 3D rapid prototyping [1-3].

In this presentation we introduce a numerical model for predicting the instability and breakup of viscous microjets of Newtonian fluid. We adopt a one-dimensional slender-jet approximation and obtain the equations of motion in the form of a system of coupled nonlinear partial differential equations (PDEs). We solve these equations using the method-of-lines (MOL), wherein the PDEs are transformed to a system of ODEs for the nodal values of the jet variables on a uniform staggered. The model accounts for arbitrary time-dependent perturbations of the free-surface, velocity and/or surface tension as boundary conditions at the nozzle orifice.

We have used the model to design continuous inkjet printing systems. In such applications, liquid microjets are modulated in a controlled fashion to create steady streams of picoliter-sized droplets at frequency rates that can exceed 500 kHz. In our lab, integrated microfluidic inkjet devices have been developed that utilize thermally modulated jets to enable color printing with unprecedented speed and versatility [4-10]. These devices consist of a pressurized reservoir that feeds a microfluidic nozzle manifold with hundreds of active orifices, each of which produces a continuous microjet of fluid. Controlled thermal modulation

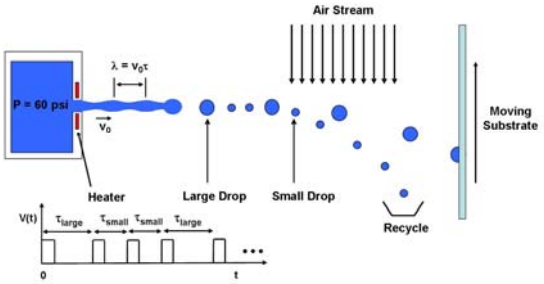

Figure 1: Illustration showing a single nozzle of an inkjet printhead with an integrated heater at the orifice, and a thermal modulation pulse used to induce different sized drop formation and air flow size selection for printing.

of each jet is achieved using CMOS/MEMS technology wherein a resistive heater element is integrated into the nozzle surrounding each orifice. To modulate a jet, a periodic voltage is applied to the heater, which causes a periodic diffusion of thermal energy from the heater into the fluid near the orifice (Fig. 1). Thus, the temperature of fluid, and hence the temperature dependent fluid properties, density, viscosity and surface tension, are modulated near the orifice. The dominant cause of jet instability is the

modulation of surface tension. To first order, the temperature dependence of σ is given by $\sigma(T) = \sigma_0 - \beta(T - T_0)$, where $\sigma(T)$ and σ_0 are the surface tension at temperatures T and T_0, respectively. The pulsed heating modulates σ at a wavelength $\lambda = v_0\tau$, where v_0 is the jet velocity and τ is the period of the heat pulse as shown in Fig. 1. The down-stream advection of thermal energy gives rise to a spatial variation (gradient) of surface tension along the jet. This produces a shear stress at the free-surface, which is balanced by inertial forces in the fluid, thereby inducing a Marangoni flow towards regions higher surface tension (from warmer regions towards cooler regions). This causes a deformation of the free-surface (slight necking in the warmer regions and ballooning in the cooler regions) that ultimately leads to instability and drop formation [4-10]. The drop volume can be adjusted on demand by varying τ, i.e., $V_{drop} = \pi r_0^2 v_o \tau$. Thus, longer pulses produce larger drops, shorter pulses produce smaller drops, and different sized drops can be produced from each orifice as desired. For printing applications two different sized drops are produced from each nozzle. The larger drops are projected onto a substrate to form an image while the smaller sized drops are deflected using air flow and recycled as shown in Fig. 1.

The design of continuous inkjet printing devices typically involves time consuming CFD analysis which can take several days for a single simulation [5-7,10]. The model presented here reduces the computation time to less than an hour and is useful for parametric design of a device.

2 EQUATIONS OF MOTION

The equations governing the behavior of a non-isothermal viscous microjet of an incompressible Newtonian fluid with surface tension σ, viscosity μ, density ρ, specific heat c_p, and thermal conductivity k, are as follows:

Navier-Stokes:

$$\rho \frac{Dv}{Dt} = -\nabla p + \mu \nabla^2 v, \tag{1}$$

where $\frac{D}{Dt} = \frac{\partial}{\partial t} + v \bullet \nabla$.

Thermal:

$$\rho c_p \frac{DT}{Dt} = k \nabla^2 T. \tag{2}$$

Continuity:

$$\nabla \bullet v = 0. \tag{3}$$

Boundary Conditions:

Thermal:

$$-k\,\hat{n} \bullet \nabla T = h_c (T - T_\infty). \tag{4}$$

Normal Stress:

$$(\mathbb{T} \bullet \hat{n}) \bullet \hat{n} = -2H\sigma. \tag{5}$$

Tangential Stress:

$$(\mathbb{T} \bullet \hat{n}) \bullet \hat{t} = \hat{t} \bullet \nabla_s \sigma. \tag{6}$$

Kinematic (at jet surface):

$$\frac{D}{Dt}\left(r_s - h(z,t)\right) = 0. \tag{7}$$

On axis (r = 0):

$$v_r = \frac{\partial v_z}{\partial r} = \frac{\partial T}{\partial r} = 0, \tag{8}$$

where v, p, and T are the velocity, pressure and temperature distributions along the microjet, v_r and v_z are the radial and axial velocity components, $h(z,t)$ defines the free-surface, $\hat{n}$ and $\hat{t}$ are unit vectors normal and tangential to the free-surface, ∇_s is the gradient operator along the free-surface, $\mathbb{T}$ is the stress tensor, and h_c is the coefficient for thermal convection off the free-surface. The function H is given by

$$H = \frac{1}{2}\left(\frac{1}{h(1+h'^2)^{1/2}} - \frac{h''}{(1+h'^2)^{3/2}} \right), \tag{9}$$

where $h' = \partial_z h$. Equations (1) - (8) need to be solved subject to appropriate boundary conditions.

3 THE MODEL

For slender microjets, equations (1)-(8) can be simplified using a perturbation expansion in r for the unknown variables h, T and v, and retaining the lowest order terms [1]. This leads to the following 1-D slender jet equations:

$$\frac{\partial v}{\partial t} + v\frac{\partial v}{\partial z} = -\frac{1}{\rho}\frac{\partial (2\sigma H)}{\partial z} + \frac{3\mu}{\rho h^2}\frac{\partial}{\partial z}\left(h^2 \frac{\partial v}{\partial z}\right) + \frac{2}{\rho h}\frac{\partial \sigma}{\partial z}, \tag{10}$$

$$\frac{\partial h^2}{\partial t} = -\frac{\partial\left(h^2 v\right)}{\partial z}, \qquad (11)$$

$$\frac{\partial T}{\partial t} + v\frac{\partial T}{\partial z} = \alpha\frac{1}{h^2}\frac{\partial}{\partial z}\left(h^2\frac{\partial T}{\partial z}\right) - \frac{2\alpha h_c}{hk}\left(T - T_\infty\right). \qquad (12)$$

In this approximation, there is thermal diffusion along the axis of the microjet and convection from its surface, but no radial thermal diffusion (1-D approximation).

We solve the slender jet equations (10) - (12) (subject to appropriate boundary conditions) using the method of lines (MOL) [10]. The MOL is typically implemented using finite differences for the spatial derivatives and ordinary differential equations for the time derivatives. We use a uniform staggered computational grid for the finite differences where h, p, and T are evaluated on one set of nodes, and the velocity v is computed on interlaced nodes midway between the first set (Fig. 2). Thus, in the MOL approach, Eq. (11) reduces to a system of N ODEs of the form

$$\frac{\partial h_i}{\partial t} = -\frac{h_{i+1/2}v_i - h_{i-1/2}v_{i-1}}{2h_i\Delta z} \qquad \left(1 \le i \le N\right) \quad (13)$$

where N is the number of nodes, and $h_{i+1/2} = \left(h_i + h_{i+1}\right)/2$ $h_{i-1/2} = \left(h_i + h_{i-1}\right)/2$. A similar system of ODEs is obtained for both Eqs. (10) and (12), and therefore a total of number of approximately 3N ODEs need to be solved for each simulation. Furthermore, one needs to apply a numerical upwind differencing scheme for the accurate solution of Eqs. (10) and (12).

We have implemented the MOL in MATLAB using the ODE solver routines for our numerical studies. We developed models to study both infinite cylinders of fluid with periodic modulation, and nozzle driven microjets

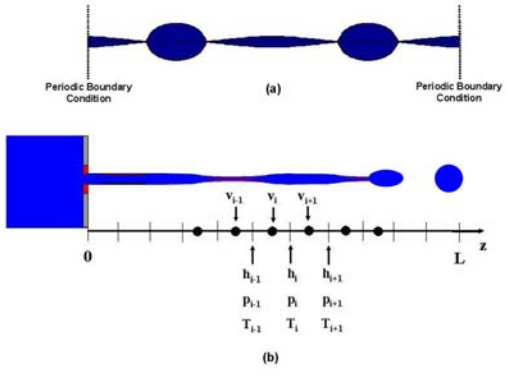

Figure 2: Staggered computational grid: (a) infinite cylinder at pinch-off with periodic boundary conditions, (b) schematic of nozzle driven microjet.

wherein the modulation is applied in a time-wise fashion at the orifice, and then convected downstream. The models take into account temperature dependent fluid properties such as surface tension.

As noted above, our model can be used to predict jet instability to breakup and beyond allowing one to track the generation of multiple sequential drops including the details of satellite formation. To implement this feature, the program breaks a fluid ligament or filament into two separate domains when the minimum jet radius reaches a prescribed threshold. Once the threshold is satisfied, the code segments the filament into two separate computational domains. Each pass of the ODE solver evolves each ligament separately before proceeding to the next time-step. Because of the uniform grid used to discretize the model, every break will remove grid points from the main filament. Thus, it is necessary to add grid points to both sides of the break using linear interpolation.

Figure 3 shows the decision-making process used in the flow of the numerical code. For each mass of fluid, there exists a separate computational domain and unique grid spacing. For each ligament and time-step, we track the following: surface height h, velocity *v*, temperature T, number of grid points N, left endpoint position B, and ligament length L. These are passed to the ODE solver where boundary conditions are applied and the equations of motion are applied for one time step. Then, the program checks for a break or merge. If one is found, the ODE solver is halted and the main program partitions or merges the data streams accordingly. Flag variables are used to communicate back to the main program which ligament(s) is breaking or merging. Then, the new stream is passed to the ODE solver to re-start the sequence. All data is saved at

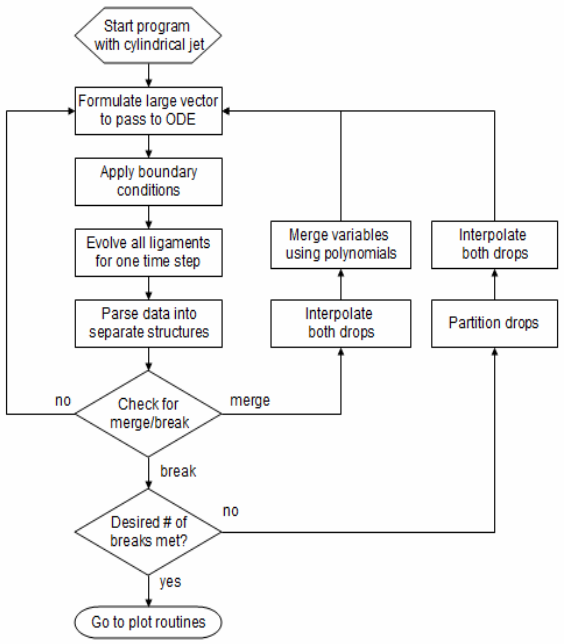

Figure 3: Flow chart of algorithm for computing

every output time step of the ODE solver. This way, we have access to the entire time history of the sequence and can plot or animate any event of our choosing.

4 RESULTS

We have used the model described above to analyze drop generation for the inkjet system shown in Fig. 1. A sample prediction of drop formation along with corresponding experimental data is shown in Fig. 4. A simulation of multiple drop formation showing satellite formation is shown in Figure 5. This simulation was completed within 30 minutes on a workstation.

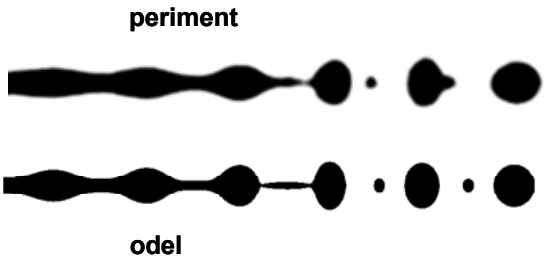

Figure 4: Comparison of predicted and observed pinch-off and drop formation.

Although the model is demonstrated here for continuous inkjet applications, it can be easily adapted for drop-on-demand printing applications.

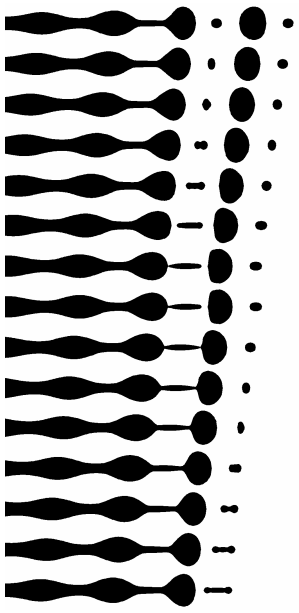

Figure 5: The formation of a satellite drop between primary drops is shown. Time is increasing from bottom to top.

5 CONCLUSIONS

We have presented a model for predicting the nonlinear deformation, pinch-off and drop generation of slender fluid cylinders and microjets. The model is easily programmed and well suited for parametric analysis. It has proven to be useful for the design and analysis of high-speed continuous inkjet printing devices.

REFERENCES

[1] Eggers J and Villermaux E. Physics of liquid jets. Rep. Prog. Phys. 2008; 71:036601.

[2] Ashley CT. Emerging applications for inkjet technology. Int. Conf. Digital Printing Tech. 2002; 18:540542.

[3] Basaran OA. Small-scale free surface flows with breakup: Drop formation and emerging applications. AIChE J. 2002; 48 9:84821848.

[4] Chwalek JM, Trauernicht DP, Delametter CN, Sharma R, Jeanmaire DL, Anagnostopoulos CN, Hawkins GA, Ambravaneswaran B, Panditaratne JC, and Basaran OA. A new method for deflecting liquid microjets. Phys. Fluids 2002; 14 6:3740.

[5] E. P. Furlani, "Temporal instability of viscous liquid microjets with spatially varying surface tension," J. Phys. A: Math. and Gen. **38**, 263-276, 2005.

[6] E. P. Furlani, "Thermal Modulation and Instability of Viscous Microjets", proc. NSTI Nanotechnology Conference 2005.

[7] E. P. Furlani, B. G. Price, G. Hawkins, and A. G. Lopez, "Thermally Induced Marangoni Instability of Liquid Microjets with Application to Continuous Inkjet Printing", Proc. NSTI Nanotechnology Conference, 2006.

[8] Z. Gao. "Instability of non-Newtonian jets with a surface tension gradient', J. Phys. A: Math. Theor. 42 065501, 2009.

[9] Z. Gao and K. C. Ng. "Analysis of power law liquid jets', Comp. and Fluids, **39 (5)**, 820-828, 2010.

[10] E. P. Furlani and M. S. Hanchak, Nonlinear Analysis of the Deformation and Breakup of Viscous Microjets using the Method of Lines, Int. J. for Numerical Methods in Fluids, on line, March 2010.